# Development and assessment of non-linear and non-stationary seasonal rainfall forecast models for the Sirba watershed, West Africa

Abdouramane Gado Djibo, Ousmane Seidou, Harouna Karambiri, Ketevera Sittichok, Jean-Emmanuel Paturel, Hadiza Moussa Saley

Journal of Hydrology: Regional Studies 4 (2015) 134–152

Contents lists available at ScienceDirect

Journal of Hydrology: Regional Studies

journal homepage: www.elsevier.com/locate/ejrh

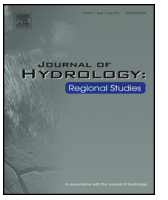

# Development and assessment of non-linear and non-stationary seasonal rainfall forecast models for the Sirba watershed, West Africa

Abdouramane Gado Djibo [a,b,*], Ousmane Seidou [b], Harouna Karambiri [a], Ketevera Sittichok [b], Jean Emmanuel Paturel [c], Hadiza Moussa Saley [d]

[a] International Institute for Water and Environmental Engineering (2iE), 01 BP 594 Ouagadougou, Burkina Faso
[b] Department of Civil Engineering, University of Ottawa, ON, Canada
[c] Institut de Recherche pour le Développement (IRD), Abidjan, Cote d'Ivoire
[d] Centre Africain d'Études Supérieures en Gestion, Dakar, Senegal

ARTICLE INFO

*Article history:*
Received 21 January 2015
Received in revised form 2 May 2015
Accepted 9 May 2015
Available online 23 June 2015

*Keywords:*
Change point detection
Seasonal rainfall forecast
Bayes factor
Sirba watershed
West Africa

ABSTRACT

**Study region:** The Sirba watershed, Niger and Burkina Faso countries, West Africa.
**Study focus:** Water resources management in the Sahel region, West Africa, is extremely difficult because of high inter-annual rainfall variability. Unexpected floods and droughts often lead to severe humanitarian crises. Seasonal rainfall forecasting is one possible way to increase resilience to climate variability by providing information in advance about the amount of rainfall expected in each upcoming rainy season. Rainfall forecasting models often arbitrarily assume that rainfall is linked to predictors by a multiple linear regression with parameters that are independent of time and of predictor magnitude. Two probabilistic methods based on change point detection that allow the relationship to change according to time or rainfall magnitude were developed in this paper using normalized Bayes factors. Each method uses one of the following predictors: sea level pressure, air temperature and relative humidity. Method M1 allows for change in model parameters according to annual rainfall magnitude, while M2 allows for changes in model parameters with time. M1 and M2 were compared to the classical linear model with constant parameters (M3) and to the climatology (M4).
**New hydrological insights for the region:** The model that allows a change in the predictor–predictand relationship according to rainfall amplitude (M1) and uses air temperature as predictor is the best model for seasonal rainfall forecasting in the study area.



* Corresponding author at: Department of Civil Engineering, University of Ottawa, ON, Canada. Tel.: +1 6136080582.
*E-mail address:* abdouramanegado@gmail.com (A. Gado Djibo).

http://dx.doi.org/10.1016/j.ejrh.2015.05.001

## 1. Introduction

Several studies show the degree to which West Africa is vulnerable to climate variability, including those by Giannini et al. (2008) and Christensen et al. (2007). The Sahelian rainfall pattern is season dependent and is directly related to the West African Monsoon (WAM) which dynamic is yet to be fully understood by climatologists (Mohino et al., 2011; Caminade and Terray, 2010; Biasutti et al., 2008; Camberlin et al., 2001; Rowell, 2001, 2003; Janicot et al., 2001; Palmer, 1986). This lack of knowledge about the WAM dynamic is part of the reason for which forecasts in the Sahel at all scales are problematic. The uncertainty in the forecasts directly affects local populations (Hayes et al., 2005). Indeed, the lack of awareness of the short and medium term evolution of rainfall and streamflows often results in populations being poorly prepare to cope with increasingly frequent climate extremes, including lack of precipitation, and floods and their direct corollaries such as lower crop yields, total loss of agricultural production or the destruction of economically valuable infrastructure, such as roads and dams (Tarhule, 2005; Samimi et al., 2012). Recurrent droughts also regularly affect agricultural production, streamflows often take authorities and largely rural local populations by surprise, despite over a decade of publication of seasonal forecasts in West Africa (*PRESAO: Prévision Saisonnière en Afrique de l'Ouest*. Hamatan, 2002; Ogallo et al., 2000). In such an unstable situation, any scientific information regarding the short (24 h) and medium (6 months) terms of rainfall and streamflow trends becomes a crucial tool for decision-making and water resources management. Agriculture, the primary socio-economic activity in the Sahelian zone, could be more efficient if, local and reliable seasonal information was available to help farmers make critical agricultural decisions (Hansen, 2002). Thus, the development of seasonal rainfall and streamflow forecast models is highly anticipated by all concerned, particularly the rural population, as it would enable effective use of climatic information that would help ensure food security. The models would increase resilience to climate variability by providing advance information about the expected amount of rain or runoff in the next rainy season (Hansen et al., 2011).

Relevant efforts of the scientific community are based on three different but complementary approaches (Hastenrath, 1995): dynamical (based purely on numerical models), statistical (based purely on statistics) and hybrid statistical-dynamical (a combination of statistics and numerical models).

The dynamical approach is based on numerical models of physics and dynamics equations that describe the climate system (Kumar et al., 1996; Brankovic and Palmer, 1997; Palmer et al., 2000, 2004). The statistical approach consists of establishing a direct relationship between the state of the atmosphere or ocean at the moment of the forecast and during event occurrences (e.g. precipitation) within the period of a few months or weeks (Schepen et al., 2012; Lopez-Bustins et al., 2008). The existence of sufficiently strong and robust physical links between certain variables is regarded as foreseeable, and is the basis of the statistical forecast. The hybrid statistical-numerical approach also known as model output statistics (MOS), is a combination method based on the principle of applying statistical methods to the output obtained from numerical models, in order to perform further analysis.

Statistical models are quite popular, given their ease of development and the limitations of dynamical models (Sittichok et al., 2014; Ibrahim et al., 2014; Mara, 2010; Bouali, 2009; Biasutti et al., 2008; Hayes et al., 2005; Philippon and Fontaine, 2002; Janicot et al., 2001; Hunt, 2000; Thiaw et al., 1999). However, it is notable that all models developed from these studies arbitrarily consider the relationship between the predictors and the predictand (rainfall in the Sahel) to be independent of time and rainfall magnitude.

The objective of this paper is to depart from that hypothesis to develop statistical seasonal rainfall forecasting models with changing parameters, and to instead compare the new models to the classical linear model with constant parameters and to the climatology.

First, a linear rainfall forecasting model is developed for each of the predictors under consideration, as in Sittichok et al. (2014). At the end of the process, an optimal lag time and optimal season are obtained to average the predictor. Using the latter lag time and the predictor time series, new models are developed that allow the linear regression parameter to change according to time or rainfall amplitude. The performance of the new models is then compared to that

of the original linear model, and to a model representing the rainfall climatology in the study area.

## 2. Materials and methods

### 2.1. Study area

The area under study considered in this work is the Sirba watershed, a transboundary watershed, shared by Burkina Faso and Niger, located between latitudes 12°55′54″–14°23′30″ N and longitudes 1°27′ W–-1°23′42″ E with an area of 38,750 km$^2$ (Mara, 2010). Fig. 1 depicts the geographical situation and characteristics of the area, which is influenced by three sub-climate zones based on the decrease of rainfall from south to north: the southern Soudanian zone with mean annual rainfall of 700–800 mm, the northern Soudanian zone with mean annual rainfall of 550–650 mm and the Sahelian zone with mean annual rainfall of 300–500 mm (Taweye, 1995). Most of rainfall occurs from July to September (JAS), regardless of the sub-climate zone. The climate is characterized in part by having only two seasons: a dry season (October to April) due to the harmattan (dry wind) and a rainy season (May to September) influenced by the WAM (cold wind) (Descroix et al., 2009). The hydrographic network is relatively dense, and consists of three main tributaries (Sirba, Faga, and Yeli) plus a few dam water reservoirs (Mara, 2010). Based on descriptions of the rainfall pattern, the hydrological regime in the Sirba watershed is the Sahelian type, and its vegetation formation is thorny, lightly wooded savannah (Andersen et al., 2005; Descroix et al., 2009). The reason for choosing the Sirba basin is threefold. First, it is located approximately in the middle of the Sahel region, so, it is influenced by the climate characteristics of both northern Sahel and the Sahara desert, and southern Sahel and the Sudanian savanna. Second, there are many climate stations inside and around the basin that collect climate data daily. And third, there is more than 40 years of precipitation data available.

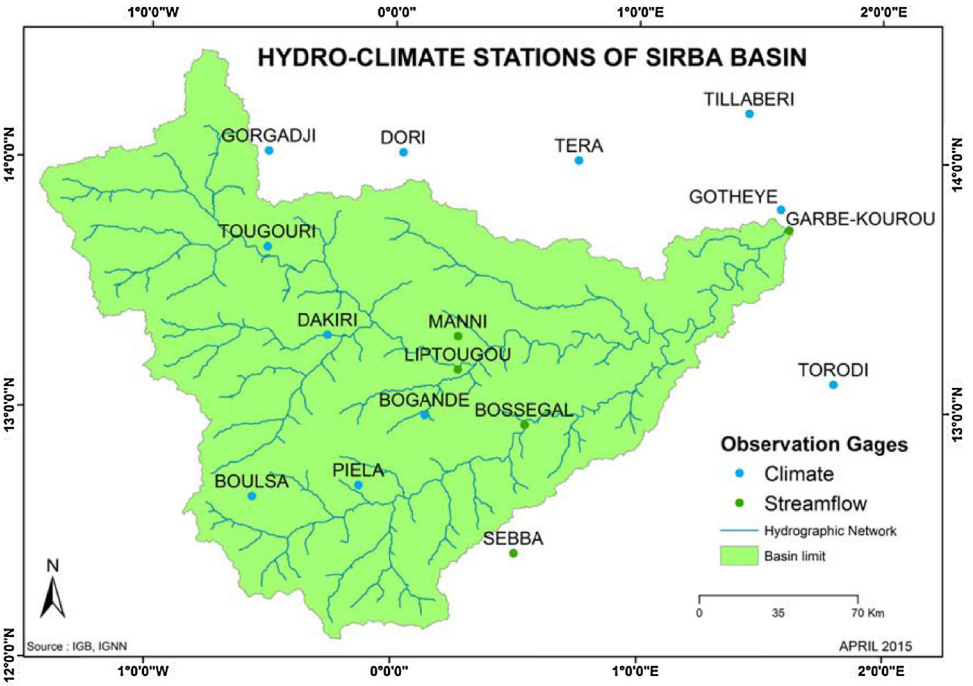


**Fig. 1.** Location map of the Sirba watershed and its hydro-meteorological stations.

**Table 1**
Details of rainfall stations.

| Station number (code) | Station name | Longitude | Latitude | Country |
|---|---|---|---|---|
| 320006 | Torodi | 1.8 | 13.12 | Niger |
| 320002 | Tera | 0.82 | 14.03 | Niger |
| 320004 | Tillaberi | 1.45 | 14.20 | Niger |
| 320005 | Gotheye | 1.58 | 13.82 | Niger |
| 200082 | Boulsa | −0.57 | 12.65 | Burkina Faso |
| 200026 | Dori | 0.033 | 14.03 | Burkina Faso |
| 200085 | Bogande | 0.13 | 12.98 | Burkina Faso |
| 200048 | Dakiri | −0.27 | 13.30 | Burkina Faso |
| 200024 | Gorgadji | −0.52 | 14.03 | Burkina Faso |
| 200086 | Piela | −0.13 | 12.70 | Burkina Faso |
| 200047 | Tougouri | −0.52 | 13.65 | Burkina Faso |

### 2.2. Climatic data

The predictand in this study is the average seasonal precipitation in the Sirba watershed. It was calculated using daily rainfall data that was recorded by a network of 11 rain gage stations in Burkina Faso and Niger, from 1960 to 2008. The rainfall time series were provided by the national meteorological offices of Burkina Faso and Niger. Five of the stations are located within the watershed, and the remaining six are a maximum of 25 km from the watershed boundary (see Fig. 1). Using the 11 rainfall time series, the Thiessen polygon method was applied to estimate the average rainfall in the watershed.

The atmospheric data are sea level pressure (SLP), relative humidity (RHUM), air temperature (AirTemp), zonal wind (UWND) and meridional wind (VWND). The variables are monthly *NCEP-DOE Reanalysis* data obtained from the National Oceanic and Atmospheric Administration (NOAA: http://www.esrl.noaa.gov). They relate to the grid 90° N–90° S latitudes and 0° E–357.5° E longitudes, and span the period from January 1979 to August 2013. Tables 1 and 2 present the rainfall and atmospheric data, respectively.

### 2.3. Selection of the optimal lag time for each predictor

Monthly precipitation time series from the Climatic Research Unit (CRU TS 3.21 0.5° global), with a spatial resolution 0.5° × 0.5° defined on 2° W–2° E longitude, and 10° N–15 °N latitude (covering more

**Table 2**
Description of climate variables.

| Parameter | Units | Level | Reference data | Spatial coverage | Temporal coverage |
|---|---|---|---|---|---|
| Sea level pressures (SLP) | Pa/s | 1000 hPa | NCEP 2 | 2.5° × 2.5° grid 90° N–90° S, 0° E–357.5° E | 1979/01/01 to 2013/08/31 |
| Air temperature (AirTemp) | K | 1000 hPa | NCEP 2 | 2.5° × 2.5° grid 90° N–90° S, 0° E–357.5° E | 1979/01/01 to 2013/08/31 |
| Relative humidity (RHUM) | % | 1000 hPa | NCEP 2 | 2.5° × 2.5° grid 90° N–90° S, 0° E–357.5° E | 1979/01/01 to 2013/08/31 |
| Meridional wind (VWND) | m/s | 1000 hPa | NCEP 2 | 2.5° × 2.5° grid 90° N–90° S, 0° E–357.5° E | 1979/01/01 to 2013/08/31 |
| Zonal wind (UWND) | m/s | 1000 hPa | NCEP 2 | 2.5° × 2.5° grid 90° N–90° S, 0° E–357.5° E | 1979/01/01 to 2013/08/31 |

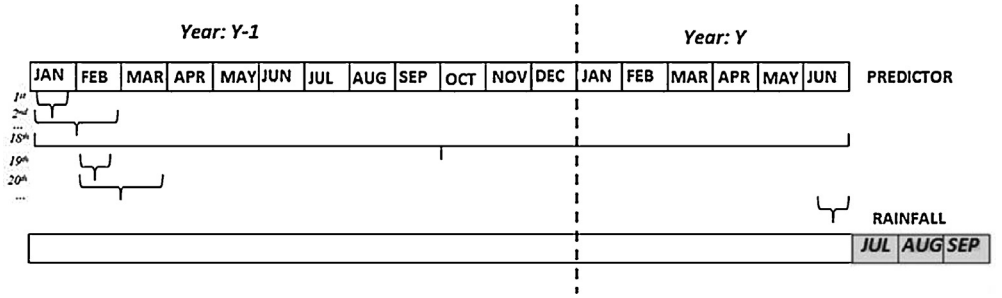


**Fig. 2.** Predictor averaging periods.

than the area of Sirba basin) were initially used as predictand for selecting a pool of potential predictors for seasonal rainfall forecasting.

After establishing the pool of predictors, the observed precipitation from rain gage stations was used to determine the best predictors in the group. The method developed by Sittichok et al. (2014) was used to link the observed rainfall with each predictor, and the candidate predictor was aggregated over all possible time windows (with a time window length in months is an integer) in the 18 months prior to the rainy season. Each of the obtained time series was used as input to a linear model linking it to the seasonal rainfall on the Sirba watershed. How the periods are generated is shown in Fig. 2. For each period, a linear model linking the predictor averaged over that period and seasonal rainfall on the Sirba is built as follows:

1. For each year $Y$ that the predictor was available.
   (i) the predictor of year $Y-1$ was removed from the predictor grid;
   (ii) the rainfall of year $Y$ was removed from the rainfall data set; and
   (iii) the dimension of the remaining predictor data set was reduced using the coefficient of determination ($R^2$) to screen predictor gridded points and obtain a small number of predictors. Principal component analysis (PCA) was then applied on the remaining predictor gridded data from the previous step to reduce the number of predictors.
2. A linear regression was fitted between the predictor and precipitation time series.
3. The fitted linear regression was used to simulate the rainfall of year $Y$. If predictor and rainfall were in the same year ($Y$), only predictor and rainfall time series for that year were removed in the first step.
4. When the simulated rainfall was available for every year in the historical period, the objective functions $R^2$, Nash, and hit-rate score were calculated to estimate the model's performance.

The period that yielded the best Nash coefficient (i.e. the optimal lag time) is then selected. Table 3 summarizes the final selected predictors used in this study to forecast seasonal rainfall.

**Table 3**
Selected predictors with their lag time for seasonal forecast.

| Predictors | NMAX[b] | $R^2$ | Nash | HIT rate score | Best periodM1–M2[a] | Lagged period |
|---|---|---|---|---|---|---|
| Sea level pressure at 1000 hPa | 50 | 0.48 | 0.46 | 60.71 | 17–18 | 0 |
| Relative humidity at 1000 hPa | 80 | 0.58 | 0.52 | 64.29 | 10–10 | 8 months |
| Air temperature at 1000 hPa | 10 | 0.530 | 0.527 | 67.86 | 1–4 | 14 months |

[a] M1 = 1:12 (January to December); M2 = M1:18 (considered month of M1 to the next coming June).
[b] NMAX: number of best grid points retained after screening the predictor grid based on $R^2$.

### 2.4. Seasonal forecasting models with changing parameters

The adapted algorithm of the Bayesian change point detection method is presented before describing the developed models with changing parameters.

#### 2.4.1. Multiple change point detection algorithm

Change points can be defined as discontinuities of time series that normally exist in climate data (Reeves et al., 2006). They can occur for many reasons, including, observed station movement, changes in recording equipment, changes in measurement techniques, environmental changes and climate change effects such as shifts in climate regimes (Lund and Reeves, 2002). There are many methods in the literature to detect and correct change points in various fields of research (Vincent, 1998; Begert et al., 2005; Beaulieu et al., 2005, 2009; Fearnhead, 2006; Seidou et al., 2007; Seidou and Ouarda, 2007; Villarini et al., 2011). Indeed, the Bayesian method for change point analysis is one of the most popular techniques, as it helps obtain the statistical distribution for the dates of change as well as the distribution for the other parameters in the model (Sarr et al., 2013; Seidou et al., 2007; Seidou and Ouarda, 2007; Xiong and Guo, 2004; Perreault et al., 2000; Gelfand et al., 1990; Barry and Hartigan, 1993). In this study, the Bayesian change point method proposed by Seidou and Ouarda (2007) is employed to evaluate abrupt changes in mean or direction of trends for climatic variables. This method was adopted because it handles an unknown number of changes and displays the complete probability distribution of the dates of the changes. The Bayesian change point detection model used in this present case can also evaluate abrupt changes in the relationship between the principal and a number of relevant explanatory variables. In these cases, the estimated trend for each segment of the time series is performed based on proxies.

A brief description of the model algorithm follows. Readers can refer to Seidou and Ouarda (2007) and Ehsanzadeh and Adamowski (2010) for further details.

Let $Y=(y_1, y_2, \ldots, y_n)$ be the $n$-sample of observations representing the response variable, $m$ be the unknown number of change points and $\tau_0=0$, $\tau_1, \ldots, \tau_{m+1}=n$. Let $Y_{t:s}$ be observations from time $t$ to time $s$; $Y_{t:s}=(y_t, y_{t+1}, y_{t+2}, \ldots, y_s)$ $(t \le s)$. Then, for $k=1, \ldots, m+1$, the $k$th segment is the set of data observed between $\tau_{k+1}+1$ and $\tau_k$. A parameter $\emptyset_k$ is associated with the $k$th segment and $\pi(\emptyset_k)$ denotes the prior distribution of $\emptyset_k$. As established by Fearnhead (2006), the posterior probability of change points is given by:

$$\begin{cases} Pr(\tau_1/Y_{1:n}) = P(1, \tau_1)Q(\tau_1+1)g_0(\tau_1)/Q(1) \\ Pr(\tau_k/\tau_{k-1}, Y_{1:n}) = P(\tau_{k-1}+1, \tau_k)Q(\tau_k+1)g(\tau_k-\tau_{k-1})/Q(\tau_{k-1}+1), \quad \text{for} \quad k=2, \ldots, m \end{cases} \tag{1}$$

where $(g)$ is the probability distribution of the time interval between two consecutive change points, and $g_0$ is the probability distribution of the first change point. For $s \ge t$ and $y_i \in Y_{t:s}$ ; $P(t, s) = \int \prod_{i=t}^{s} f(y_i/\theta)\pi(\theta)d\theta$ is the probability of $t$ and $s$ belonging to the same segment. $Q(t)$ is the likelihood of segment $Y_{t:n}$ given a change point at $t-1$, and is derived from a recursive relation using $P(t, s)$ and both $g$ and $g_0$ (see Theorem 1, Fearnhead, 2006).

Now, let $X=(x_{1j}, x_{2j}, \ldots, x_{nj})$, and $j=1, \ldots, d^*$ denote the set of $d^*$ explanatory vectors including any intercepts. Thus, the multiple linear regression can be written as:

$$y_i = \sum_{j=1}^{d^*} \theta_j x_{ij} + \varepsilon_i, \quad i=1, \ldots, n \quad \text{or} \quad Y = X\theta + \varepsilon \tag{2}$$

where $\theta=(\theta_1, \theta_2, \ldots, \theta_{d^*})$ is the vector of the regression parameters and $\varepsilon=(\varepsilon_1, \varepsilon_2, \ldots, \varepsilon_{d^*})$ is the Gaussian vector of residuals with mean zero and variance $\sigma^2$. Note that relation (1) changes after each change point and is recomputed for each segment. In a given segment, the parameter vector $\emptyset$ is defined as:

$$\emptyset = (\theta_1, \theta_2, \ldots, \theta_{d^*}, \sigma) \tag{3}$$

and it follows that:

$$f(y_i/\emptyset) = \frac{1}{\sigma\sqrt{2\pi}} \exp\left(-0.5\left(\frac{y_i - \sum_{d^*}^{j=1}\theta_j x_{ij}}{\sigma}\right)^2\right) \tag{4}$$

In this study, the prior distribution to be used depends only on the scale parameter $\sigma$ and as such:

$$\pi_1(\emptyset) = \pi_1(\sigma) = p(\sigma/a, c) = \frac{\sigma^{-a}\exp\left(-\frac{c}{2\sigma^2}\right)}{2^{(a-3)/2}c^{(a-1)/2}\Gamma\left(\frac{a-1}{2}\right)} \quad a > 1, \quad c > 0 \tag{5}$$

where $a$ and $c$ are the hyper parameters. Hence, as shown in Seidou and Ouarda (2007), in this setting the posterior probability of the change point displayed in Eq. (1) is given by:

$$P(t,s) = (2\pi)^{d^*/2}\frac{(\pi(\varepsilon_{t:s}^T\varepsilon_{t:s} + c))^{(s-t+a-1)/2}\Gamma\left(\frac{s-t+a-d^*}{2}\right)}{(c\pi)^{(a-1)/2}\left|X_{t:s}^T X_{t:s}\right|^{1/2}\Gamma\left(\frac{a-1}{2}\right)} \quad \text{for} \quad s \geq t \tag{6}$$

In this study, parameter $a$ in Eq. (6) is fixed at 2, so that the prior distribution is non-informative.

The Bayesian change point detection model first estimates the posterior distribution of probability of the number of changes. The most probable number of detected changes (associated with the highest probability of occurrence) is then selected as the number of change points observed in the data series. Conditional on this number, the Bayesian inference then provides the time position of detected changes and their respective (posterior) distribution of probability of occurrence. Finally, the magnitude of the detected changes is determined. The identified changes could represent shifts in the mean, changes in the direction of a trend, or a combination of both.

### 2.4.2. Model M1

Model M1 was developed to detect potential changes in the relation between predictor and predictand and assumes that the relationship changes with precipitation amplitude. To obtain the forecast for a given year $i$ ($i$ = 1979–2002) the model is applied as follows:

1. Year $i$ is removed from the predictor and predictand time series.
2. Stepwise regression is used to fit a linear relation between the predictor and the predictand in the remainder of the series, and an initial forecast assuming a single equation for all points is issued. The equation is also used to issue an initial forecast for year $i$.
3. The data is sorted in increasing order of the forecasted predictand from step 2, and a new position $i_1$ is assigned to year $i$. The initial forecast for year $i$ is between the initial forecast for year $i_1$ and the initial forecast for year $i_1 + 1$.
4. The change point detection method by Seidou et al. (2007) is applied to the remaining data. The method generates 1000 time series of length $N-1$, with a random number of change points at random locations. The density of the change points in a given time interval is proportional to the probability of change in that interval (Seidou et al., 2007).
5. For each of the 1000 generated sequences of change points, stepwise regression is applied to fit a linear relation between the predictor and predictand on any segments delineated by the change points, and, both the optimal (least square) forecast and the standard deviation of the residual are calculated. If $m$ is the order of the current generated sequence of change points, $i$ is in the $k$th segment, $x_1, x_2, \ldots, x_n$ the values of the predictors for year $i$ and $\propto_1^{k,m}, \propto_2^{k,m}, \ldots, \propto_n^{k,m}$ are the coefficients of the equation for the segment $k$, then the least square estimate is $\hat{Y}_i = \propto_0^{k,m} + \propto_1^{k,m} \times x_1 + \propto_2^{k,m} \times x_2 + \cdots + \propto_n^{k,m} \times x_n$.
6. Ten probabilistic forecasts are generated by sampling ten values from a normal distribution. The mean of the normal distribution is the least square forecast and its standard deviation is the standard deviation of the forecasts.

7. The 10,000 forecasts for year *i* are used to calculate the empirical probability density of the forecast. The estimate of the distribution is nonparametric, uses a normal kernel function, and is evaluated at 1000 equally spaced points that cover the range of the data set.

At the end of the process, a probability density function is obtained for the forecast in year *i*.

*2.4.3. Model M2*

Model M2 is similar to M1, except that it assumes that the predictand–predictor relationship changes with time (i.e., the regression parameters change over time). The same approach as in M1 was followed, but there was no ordering of the data set after each exclusion of year *i* (*i* = 1979–2002).

1. Year *i* is removed from the predictor and predictand time series.
2. The Seidou et al. (2007) change point detection method is applied to the remaining data. The method generates 1000 time series of length $N-1$, with a random number of change points at random locations. The density of change points in a given time interval is proportional to the probability of change in that interval (Seidou et al., 2007).
3. For each of the 1000 generated sequences of change points, stepwise regression is applied to fit a linear relation between the predictor and predictand on any segments defined by the change points. Both the optimal (least square) forecast and the standard deviation of the residual are calculated. If $m$ is the order of the current generated sequence of change points, $i$ is in the $k$th segment, $x_1, x_2, \ldots, x_n$, and the values of the predictors for year $i$ and $\propto_1^{k,m}, \propto_2^{k,m}, \ldots, \propto_n^{k,m}$ are the coefficients of the equation for segment $k$, then the least square estimate is $\hat{Y}_i = \propto_0^{k,m} + \propto_1^{k,m} \times x_1 + \propto_2^{k,m} \times x_2 + \cdots + \propto_n^{k,m} \times x_n$.
4. Ten probabilistic forecasts are generated by sampling ten values from a normal distribution. The mean of the normal distribution is the least square forecast and its standard deviation is the standard deviation of the forecasts.
5. The 10,000 forecasts for year *i* are used to calculate the empirical probability density of the forecast. The estimate of the distribution is nonparametric, uses a normal kernel function, and is evaluated at 1000 equally spaced points that cover the range of the data set.

At the end of the process, a probability density function is obtained for the forecast in year *i* (*i* = 1979–2002).

Fig. 3 recapitulates the steps involved in the models M1 and M2.

*2.5. Seasonal forecasting models with constant parameters*

Two models with constant parameters were developed and tested in order to find the best seasonal rainfall forecast model. The first method (M3) is the classical linear model with constant parameters, and the second (M4) is based on the climatology.

*2.5.1. Model M3*

In model M3, no change points are assumed in the linear regression between predictand and predictors. The model M3 is applied as follows (see Fig. 4):

1. Year *i* is removed from the predictor and predictand time series.
2. Stepwise regression is used to fit a linear relation between the predictor and predictand. Both the optimal (least square) forecast and the standard deviation of the residual are calculated. If $i$ is in the $k$th segment, $x_1, x_2, \ldots, x_n$, and the values of the predictors for year $i$ and $\propto_1^k, \propto_2^k, \ldots, \propto_n^k$ are the coefficients of the equation for the segment containing $i$, then the least square estimate for year $i$ is $\hat{Y}_i = \propto_0^k + \propto_1^k \times x_1 + \propto_2^k \times x_2 + \cdots + \propto_n^k \times x_n$.
3. Ten probabilistic forecasts are generated by sampling ten values from a normal distribution. The mean of the normal distribution is the least square forecast and its standard deviation is the standard deviation of the forecasts.

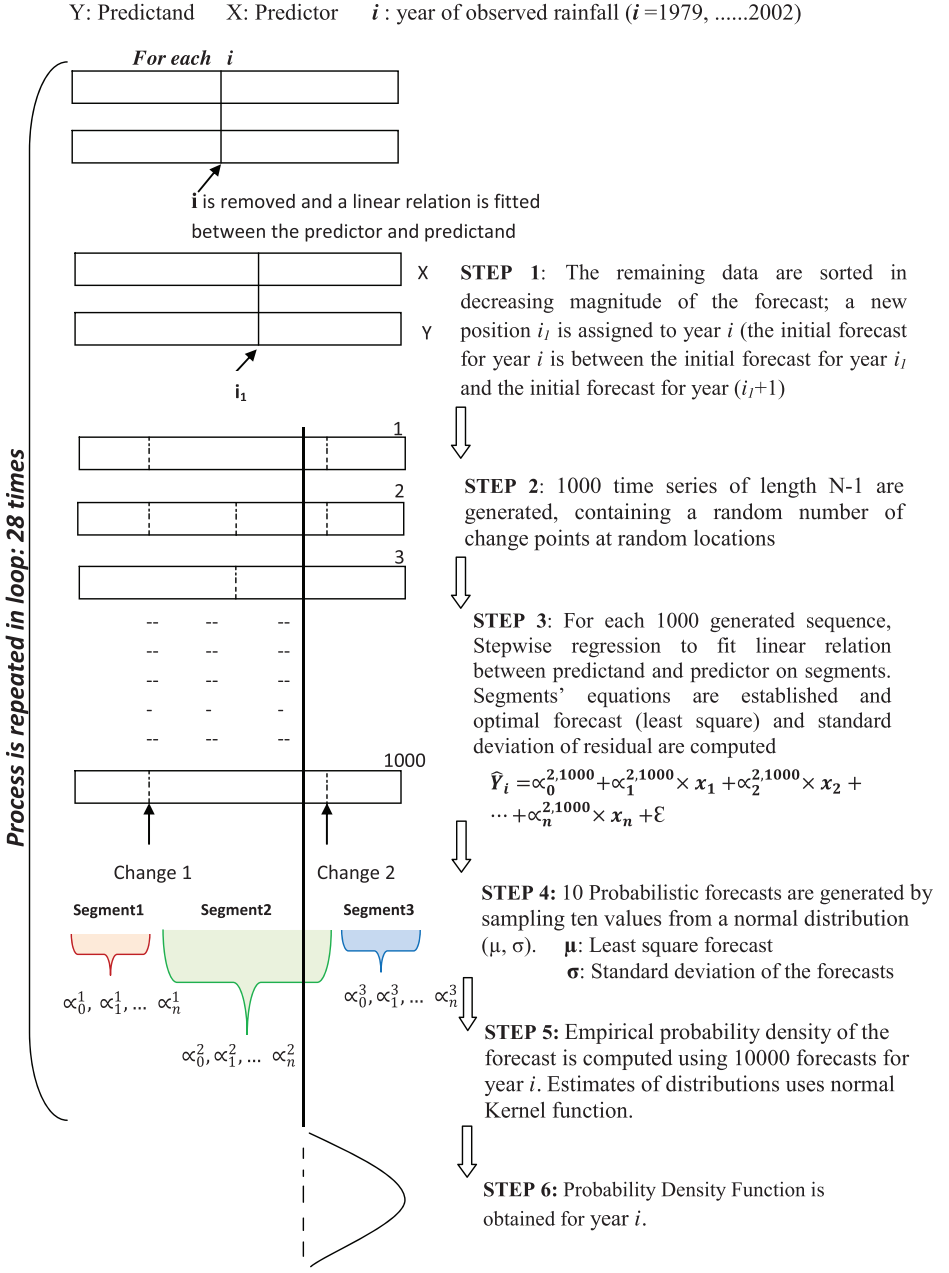


**Fig. 3.** Steps in seasonal rainfall forecasting models with changing parameters. (All steps are followed except step 1 which is not included while using model M2.)

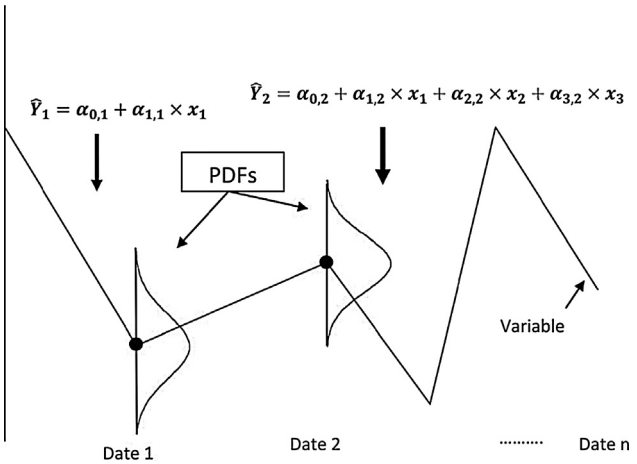


**Fig. 4.** Graphical description of model M3.

4. The 10,000 forecasts for year *i* are used to calculate the empirical probability density of the forecast. The estimate of the distribution is non-parametric, uses a normal Kernel function, and is evaluated at 1000 equally spaced points that cover the range of the data set.

At the end of the process, a probability density function is obtained for the forecast in year *i* (*i* = 1979–2002).

*2.5.2. Model M4*

Under model M4, the climatology is used to estimate the seasonal rainfall. The probability density of the forecast is a normal distribution in which the average observed precipitation is the mean and the standard deviation is the standard deviation of the observed precipitation (see Fig. 5). Model M4 is applied as follow:

1. Year *i* is removed from the predictor and predictand time series.
2. The average and the standard deviation of the observed precipitation are calculated on the remainder of the data.

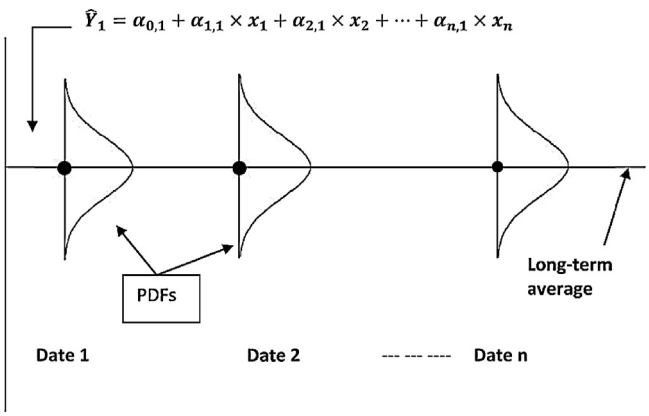


**Fig. 5.** Schematically presentation of model M4 using climatology.

3. The probability distribution of the forecast is generated at 1000 points over the range of the data, using a normal distribution. The mean of the normal distribution is the average observed precipitation, and the standard deviation is the standard deviation of the observed precipitations.
4. The 10,000 forecasts for year *i* are used to calculate the empirical probability density of the forecast. The estimate of the distribution is nonparametric, uses a normal kernel function, and is evaluated at 1000 equally spaced points over the range of the data set.

At the end of the process, a probability density function is obtained for the forecast in year *i*.

### 2.6. Bayesian model selection

In this paper, the Bayesian approach is used to select the best seasonal rainfall forecast model from developed models with changing parameters and those with constant parameters. The posterior and prior probabilities of the models and the observed data were computed first (see Eq. (1)).

$$Posterior\ Prob_{model} = \frac{(Prior\ Prob_{model} \times Likelihood_{model})}{Prob_{observations}} \tag{7}$$

where $Likelihood_{model} = \prod_{i=1}^{n} likelihood_i$, $i$ is the year of forecasted rainfall, and $n$ is the number of years.

To apply Eq. (7), all twelve models (i.e. M1, M2, M3, and M4 used with each of the three predictors) were considered. The ratio of a model's posterior probability to observations constitutes a comparative criterion after normalization. Normalized Bayes factors $B_f$ (see Eq. (8)) were calculated for each model to facilitate comparison between the models' results, and to provide a weighted comparison of the likelihood of each model given the observed data. $B_f$ compares the posterior likelihood of data $d$ of a given model $M_i$ to that of the reference model $M_r$. For more details about Bayes factors, refer to Min et al. (2007).

$$B_f = \frac{Likelihood(d/M_i)}{Likelihood(d/M_r)} \tag{8}$$

Selection of the best seasonal rainfall forecast model required analysis of the Bayes factors for all 12 models. Table 5 demonstrates how to interpret Bayes factor. There is strong evidence favorably supporting model $M_r$ (a reference model) and $M_i$ (a given model), when $B_f$ is less than 1/10 and higher than10, respectively. In contrast, $B_f$ between 1/3 and 3, meant that both the $M_r$ and $M_i$ models are weak models. Hence, the best forecast model is the one for which $B_f$ is always favorable in terms of value. In addition, the evolution of likelihoods of forecasted seasonal precipitation (JAS) was confirmed via a graphical representation of each model. The graphs show the likelihood of each forecasted rainfall value on a colored scale, where red and blue represent a probability of 1 and 0, respectively.

The entire methodology used in this work is summarized by the flowchart presented in Fig. 6.

### 2.7. Performance measures

In this study, the relative performances of the four rainfall seasonal forecasting models (M1, M2, M3 and M4) were compared quantitatively using the Nash–Sutcliffe criterion (Nash). This criterion was chosen because it can present the differences in magnitude between observed and simulated data during the entire time period. The best Nash value equates to the best performance.

The performance of each model (under each predictor) was further evaluated based on two other criteria: (i) the number of forecasted values per model with high likelihoods (e.g. 80–100%); and (ii) the model's performance if the data support it favorably, based on Bayes factors; if so it is deemed to have credible high performance.

Therefore, the model is considered to perform better if almost 100% of its forecasted values have high likelihoods, which is clearly indicated by the red plot on the graph. The opposite (i.e., low likelihoods) is plotted in blue.

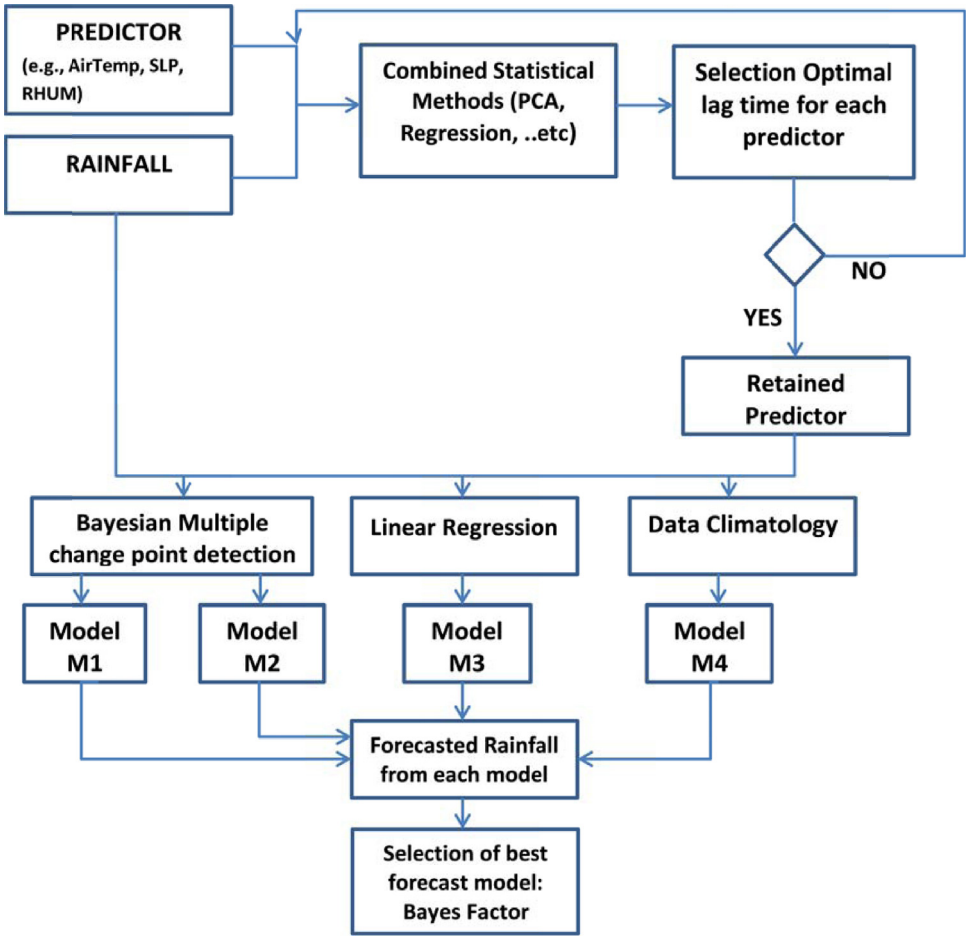


**Fig. 6.** Selection process of best seasonal rainfall forecast model.

## 3. Results and discussions

### 3.1. Changes in relationship

It was found that the linear relation between the predictor and predictand systematically displayed the presence of one or more change points. The probability of change, as well as the conditional probability of the change points, was calculated according to the work of Seidou and Ouarda (2007). Table 4 summarizes the number of change points and their respective locations for each model. It was observed that the number of change points varies between models. Fig. 7 shows the output of model M1 as a histogram representing the probability of occurrence of the first change in the data, in the case of AirTemp. The weight at the first date (position) is the probability of no change. Clearly, the effectively localized histogram indicates that the position of the change is well identified. It was assumed that no change occurs when the weight is above 0.5, and, when the probability of change is above 0.5, the position of the change was assumed to be beyond the first year that had the highest probability. Thus, in Fig. 7 at year 1990 (lower panel at position 12) it was observed that the probability of change is 55%, and the probability of no change is 45%. The conditional probability of the existing change point is also given, and shows there is a 60% chance of change at position 12.

**Table 4**
Number of change points and their most probable locations for each model.

| Models | Number of change points | Position of changes |
|---|---|---|
| $M1_a$ | 1 | 1992 |
| $M1_{rh}$ | 1 | 1990 |
| $M1_s$ | 1 | 1990 |
| $M2_a$ | 1 | 1990 |
| $M2_{rh}$ | 1 | 1990 |
| $M2_s$ | 1 | 1992 |

a: subscript for model developed using AirTemp as predictor.
rh: subscript for model developed using RHUM as predictor.
s: subscript for model developed using SLP as predictor.

### 3.2. Performance of forecasting models

The relative performance of the four rainfall seasonal forecasting models described in Sections 2.4 and 2.5 was obtained using the observed and forecasted seasonal time series. The results showed Nash values of 0.76, 0.52, 0.46 and 0.58 for models M1, M2, M3 and M4 respectively. Since the objective function used to present the forecast skill is Nash, the best performance equates to the best Nash, which indicated that model M1 outperformed the others, followed by model M4.

The limitations of model M3 could be because, unlike the Nash criteria, regression is not suitable for measuring the difference in magnitude of both the observed and simulated data. As for model M2, its limitations are the result of the imposed condition that makes the rainfall-predictor relationship change over time. Models M1 and M4 seems to perform acceptably.

Considering the performance of the models under each of the three predictors, it is interesting that for the models using AirTemp as the predictor, 92%, 38%, 81%, and 54% of the forecasted values have high likelihoods for models M1, M2, M3 and M4, respectively. Thus, the strongest model is $M1_a$, followed by $M3_a$, $M4_a$ and $M2_a$. For models using RHUM as the predictor, the performance of the models in decreasing order is $M1_{rh}$, $M4_{rh}$, $M2_{rh}$, and $M3_{rh}$, as they have 86%, 79%, 29%, and 28% of forecasted values with high likelihoods, respectively. For the last predictor SLP, the performance of

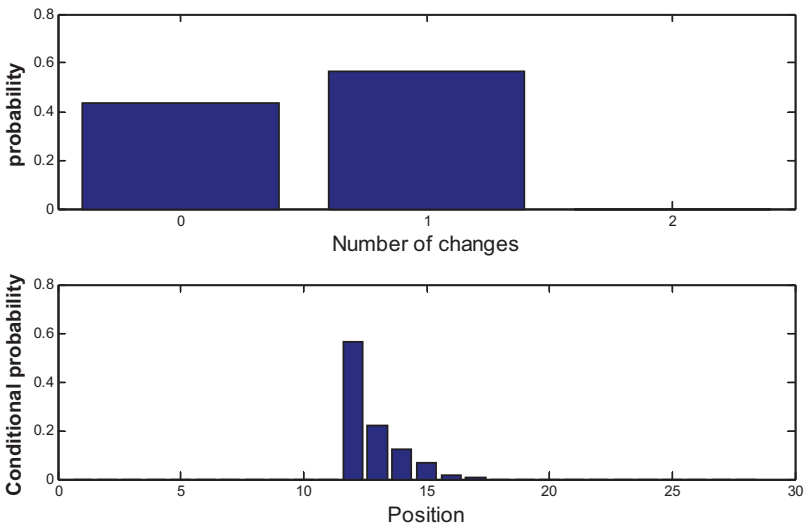


**Fig. 7.** Histogram of change point detection result for model M1.

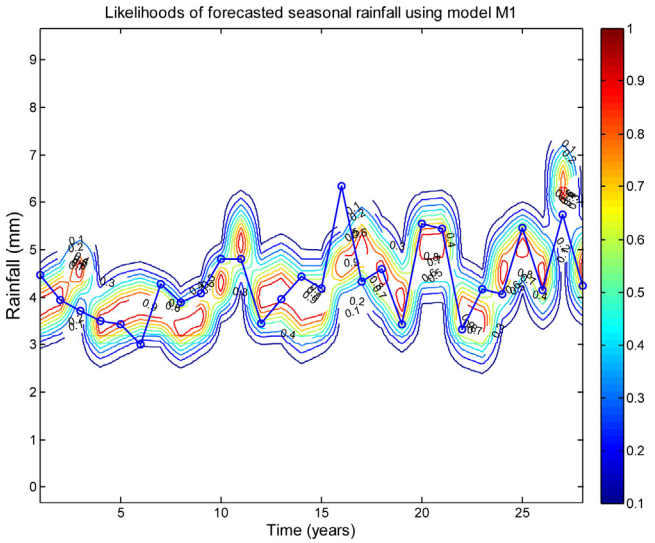


**Fig. 8.** Evolving probabilities of forecasted seasonal rainfall from M1 using AirTemp.

each model is shown by the inequalities $M4_S > M1_S > M2_S > M3_S$, as models M1, M2, M3, and M4 have 86%, 59%, 36%, and 89% of forecasted values have high likelihoods, respectively.

### 3.3. Selection of the best model

Selection of the best seasonal rainfall forecast model involved analyzing the Bayes factors for all model combinations, and visually examining the location of seasonal (JAS) precipitation on a graphical representation of each model's posterior likelihood. If the observations are largely in areas of high likelihood according to a given model, that model is deemed credible. Figs. 8–10 present the graphs for models M1, M2 and M3. On each graph, some rainfall values were in the red range (high probability) and others were in the blue range (low probability). Analysis of the evolving likelihoods (Fig. 8) found

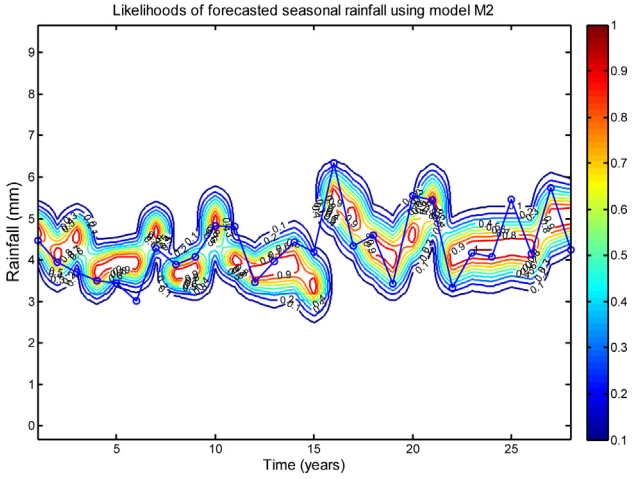


**Fig. 9.** Evolving probabilities of forecasted seasonal precipitations from M2 using RHUM.

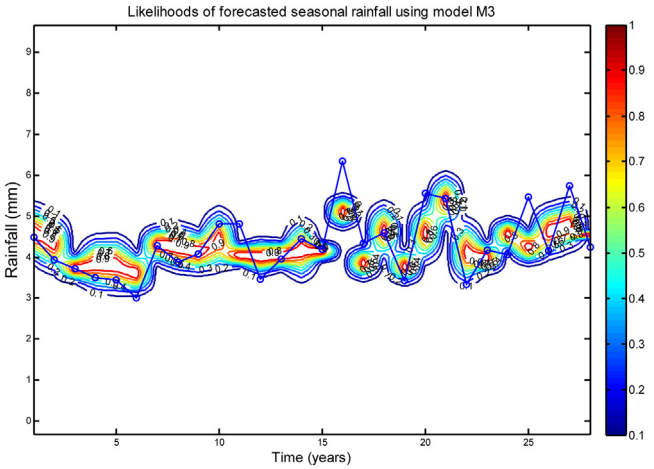


**Fig. 10.** Evolving probabilities of predicted seasonal precipitations from model M3 using SLP.

**Table 5**
Scale for Bayes factor interpretation.

| Bayes factor | Interpretation |
|---|---|
| $B_f < 1/10$ | Strong evidence for $M_r$ |
| $1/10 \leq B_f < 1/3$ | Moderate evidence for $M_r$ |
| $1/3 \leq B_f < 1$ | Weak evidence for $M_r$ |
| $1 \leq B_f < 3$ | Weak evidence for $M_i$ |
| $3 \leq B_f < 10$ | Moderate evidence for $M_i$ |
| $B_f \geq 10$ | Strong evidence for $M_i$ |

*Source*: Min et al. (2007).

that 22 of the 28 forecasted rainfall values under model M1 using AirTemp are in the red range, which indicates high probability.

Figs. 9 and 10 show the evolving likelihoods of forecasted seasonal precipitation for models M2 and M3, respectively. On these graphs, most of the forecasted seasonal rainfalls tend toward blue (i.e. low probability). In models M2 and M3, only 29% and 36% of the observations fall in areas of high likelihood respectively, so the models are deemed not credible.

Table 6 displays the normalized Bayes factors for all models. Table 5 shows how to interpret the magnitude of the Bayes factors, and concludes that there is weak, moderate or strong evidence to support the competing models. Table 7 shows that there is a strong evidence for Model M1, using AirTemp as predictor. Bayes factors favorably supported model M1 (AirTemp) because it had strong evidence (St.E) either as reference or given model, compared to the others which had moderate or weak evidence as in Table 7. Thus, for seasonal rainfall forecasts, evaluating changes in the relationship of predictand–predictor with the rainfall amplitude seems to be the best approach for the Sahelian region.

Thus, seasonal forecast models with parameters that change according to rainfall magnitude could be considered optimal for seasonal rainfall forecast over the Sirba watershed, rather than classical models where parameters are constant Combining this changing parameter model with the Bayesian change point detection procedure, and using the normalized Bayes factor, constitutes an acceptable means of forecasting seasonal rainfall over West Africa, and address an issue that has challenged forecasters for more than two decades.

**Table 6**
Normalized Bayes factors of twelve seasonal rainfall forecast models.

| $M_r$ | $M_i$ | | | | | | | | | | | |
|---|---|---|---|---|---|---|---|---|---|---|---|---|
| | AirTemp | | | | RHUM | | | | SLP | | | |
| | $M1_a$ | $M2_a$ | $M3_a$ | $M4_a$ | $M1_{rh}$ | $M2_{rh}$ | $M3_{rh}$ | $M4_{rh}$ | $M1_s$ | $M2_s$ | $M3_s$ | $M4_s$ |
| *AirTemp* | | | | | | | | | | | | |
| $M1_a$ | 1 | 8.62E−05 | 2.53E+00 | 5.53E−04 | 9.53E−02 | 1.19E−14 | 4.63E−20 | 5.53E−04 | 6.09E−06 | 8.82E−12 | 5.91E−23 | 5.53E−04 |
| $M2_a$ | 1.16E+04 | 1 | 2.94E+04 | 6.41E+00 | 1.11E+03 | 1.38E−10 | 5.37E−16 | 6.41E+00 | 7.07E−02 | 1.02E−07 | 1.74E−18 | 6.41E+00 |
| $M3_a$ | 3.95E−01 | 3.41E−05 | 1 | 2.18E−04 | 3.77E−02 | 4.69E−15 | 1.83E−20 | 2.18E−04 | 2.41E−06 | 3.48E−12 | 1.50E−22 | 2.18E−04 |
| $M4_a$ | 1.81E+03 | 1.56E−01 | 4.58E+03 | 1 | 1.72E+02 | 2.15E−11 | 8.37E−17 | 8.65E−01 | 1.10E−02 | 1.60E−08 | 2.71E−19 | 1.00E+00 |
| *RHUM* | | | | | | | | | | | | |
| $M1_{rh}$ | 1.05E+01 | 9.04E−04 | 2.66E+01 | 5.80E−03 | 1 | 1.24E−13 | 4.85E−19 | 5.80E−03 | 6.40E−05 | 9.25E−11 | 1.57E−21 | 5.80E−03 |
| $M2_{rh}$ | 8.43E+13 | 7.27E+09 | 2.13E+14 | 4.66E+10 | 8.03E+12 | 1 | 3.90E−06 | 4.66E+10 | 5.14E+08 | 7.43E+02 | 1.26E−08 | 4.66E+10 |
| $M3_{rh}$ | 2.16E+19 | 1.86E+15 | 5.47E+19 | 1.19E+16 | 2.06E+18 | 2.56E+05 | 1 | 1.19E+16 | 1.32E+14 | 1.91E+08 | 3.23E−03 | 1.19E+16 |
| $M4_{rh}$ | 2.09E+03 | 1.80E−01 | 5.29E+03 | 1.00E+00 | 1.99E+02 | 2.48E−11 | 9.67E−17 | 1 | 1.27E−02 | 1.84E−08 | 3.13E−19 | 1.00E+00 |
| *SLP* | | | | | | | | | | | | |
| $M1_s$ | 1.64E+05 | 1.41E+01 | 4.15E+05 | 9.07E+01 | 1.56E+04 | 1.95E−09 | 7.59E−15 | 9.07E+01 | 1 | 1.45E−06 | 2.45E−17 | 9.07E+01 |
| $M2_s$ | 1.13E+11 | 9.77E+06 | 2.87E+11 | 6.27E+07 | 1.08E+10 | 1.35E−03 | 5.25E−09 | 6.27E+07 | 6.91E+05 | 1 | 1.70E−11 | 6.27E+07 |
| $M3_s$ | 1.69E+22 | 5.76E+17 | 6.69E+21 | 3.69E+18 | 6.37E+20 | 7.93E+07 | 3.09E+02 | 3.69E+18 | 4.08E+16 | 5.89E+10 | 1 | 3.69E+18 |
| $M4_s$ | 1.40E+03 | 1.21E−01 | 3.54E+03 | 1.00E+00 | 1.33E+02 | 1.66E−11 | 6.47E−17 | 1.00E+00 | 8.53E−03 | 1.23E−08 | 2.09E−19 | 1 |

a: subscript for model developed using AirTemp as predictor.
rh: subscript for model developed using RHUM as predictor.
s: subscript for model developed using SLP as predictor.

**Table 7**
Comparison of twelve seasonal rainfall forecast models.

| $M_r$ | $M_i$ | | | | | | | | | | | |
|---|---|---|---|---|---|---|---|---|---|---|---|---|
| | AirTemp | | | | RHUM | | | | SLP | | | |
| | $M1_a$ | $M2_a$ | $M3_a$ | $M4_a$ | $M1_{rh}$ | $M2_{rh}$ | $M3_{rh}$ | $M4_{rh}$ | $M1_s$ | $M2_s$ | $M3_s$ | $M4_s$ |
| *AirTemp* | | | | | | | | | | | | |
| $M1_a$ | Wk.E. $M1_a$ | St.E. $M1_a$ | St.E. $M1_a$ | St.E. $M1_a$ | St.E. $M1_a$ | St.E. $M1_a$ | St.E. $M1_a$ | St.E. $M1_a$ | St.E. $M1_a$ | St.E. $M1_a$ | St.E. $M1_a$ | St.E. $M1_a$ |
| $M2_a$ | St.E. $M1_a$ | Wk.E. $M2_a$ | St.E. $M3_a$ | Md.E. $M4_a$ | St.E. $M1_{rh}$ | St.E. $M2_a$ | St.E. $M3_{rh}$ | Md.E. $M4_{rh}$ | St.E. $M2_a$ | St.E. $M2_a$ | St.E. $M2_a$ | Md.E. $M4_s$ |
| $M3_a$ | St.E. $M1_a$ | St.E. $M3_a$ | Wk.E. $M3_a$ | St.E. $M3_a$ | St.E. $M1_{rh}$ | St.E. $M2_{rh}$ | St.E. $M3_a$ | St.E. $M3_a$ | St.E. $M1_s$ | St.E. $M3_a$ | St.E. $M3_s$ | St.E. $M3_a$ |
| $M4_a$ | St.E. $M1_a$ | Md.E. $M4_a$ | St.E. $M3_a$ | Wk.E. $M4_a$ | St.E. $M1_{rh}$ | St.E. $M4_a$ | St.E. $M4_a$ | Wk.E. $M4_a$ | St.E. $M4_a$ | St.E. $M4_a$ | St.E. $M3_s$ | Wk.E. $M4_a$ |
| *RHUM* | | | | | | | | | | | | |
| $M1_{rh}$ | St.E. $M1_a$ | St.E. $M1_{rh}$ | St.E. $M1_{rh}$ | St.E. $M1_{rh}$ | Wk.E. $M1_{rh}$ | St.E. $M1_{rh}$ | St.E. $M1_{rh}$ | St.E. $M1_{rh}$ | St.E. $M1_s$ | St.E. $M1_{rh}$ | St.E. $M3_s$ | St.E. $M1_{rh}$ |
| $M2_{rh}$ | St.E. $M1_a$ | St.E. $M2_a$ | St.E. $M2_{rh}$ | St.E. $M4_a$ | St.E. $M1_{rh}$ | Wk.E. $M2_{rh}$ | St.E. $M2_{rh}$ | St.E. $M4_{rh}$ | St.E. $M1_s$ | St.E. $M2_{rh}$ | St.E. $M3_s$ | St.E. $M4_s$ |
| $M3_{rh}$ | St.E. $M1_a$ | St.E. $M3_{rh}$ | St.E. $M3_a$ | St.E. $M4_a$ | St.E. $M1_{rh}$ | St.E. $M2_{rh}$ | Wk.E. $M3_{rh}$ | St.E. $M3_{rh}$ | St.E. $M1_s$ | St.E. $M2_s$ | St.E. $M3_{rh}$ | St.E. $M4_s$ |
| $M4_{rh}$ | St.E. $M1_a$ | Md.E. $M4_{rh}$ | St.E. $M3_a$ | Wk.E. $M4_a$ | St.E. $M1_{rh}$ | St.E. $M4_{rh}$ | St.E. $M3_{rh}$ | Wk.E. $M4_{rh}$ | St.E. $M4_{rh}$ | St.E. $M4_{rh}$ | St.E. $M3_s$ | Wk.E. $M4_{rh}$ |
| *SLP* | | | | | | | | | | | | |
| $M1_s$ | St.E. $M1_a$ | St.E. $M2_a$ | St.E. $M1_s$ | St.E. $M4_a$ | St.E. $M1_s$ | St.E. $M1_s$ | St.E. $M1_s$ | St.E. $M4_{rh}$ | Wk.E. $M1_s$ | St.E. $M1_s$ | St.E. $M1_s$ | St.E. $M4_s$ |
| $M2_s$ | St.E. $M1_a$ | St.E. $M2_a$ | St.E. $M3_a$ | St.E. $M4_a$ | St.E. $M1_{rh}$ | St.E. $M2_{rh}$ | St.E. $M2_s$ | St.E. $M4_{rh}$ | St.E. $M1_s$ | Wk.E. $M2_s$ | St.E. $M2_s$ | St.E. $M4_s$ |
| $M3_s$ | St.E. $M1_a$ | St.E. $M2_a$ | St.E. $M3_s$ | St.E. $M3_s$ | St.E. $M3_s$ | St.E. $M3_s$ | St.E. $M3_{rh}$ | St.E. $M3_s$ | St.E. $M1_s$ | St.E. $M2_s$ | Wk.E. $M3_s$ | St.E. $M4_s$ |
| $M4_s$ | St.E. $M1_a$ | Md.E. $M4_s$ | St.E. $M3_a$ | Wk.E. $M4_a$ | St.E. $M1_{rh}$ | St.E. $M4_s$ | St.E. $M4_s$ | Wk.E. $M4_{rh}$ | St.E. $M4_s$ | St.E. $M4_s$ | St.E. $M4_s$ | Wk.E. $M4_s$ |

St.E.: strong evidence (for example, St.E. $M1_a$: strong evidence for $M1_a$); Md.E.: moderate evidence; Wk.E.: weak evidence.
a: subscript for model developed using AirTemp as predictor.
rh: subscript for model developed using RHUM as predictor.
s: subscript for model developed using SLP as predictor.

## 4. Conclusion

Seasonal forecast models, with either changing parameters or constant parameters, were developed and tested in this study, using three predictors (air temperature, sea level pressure and relative humidity). Normalized Bayes factors, and graphs of the likelihood of forecasted rainfall under each model, were compared. It was found that the best seasonal rainfall forecast model uses air temperature as the predictor and allows parameter changes according to rainfall magnitude. Thus, seasonal forecast models with changing parameters could be the best for seasonal rainfall forecasting in the Sirba watershed. Indeed, changes in the predictand–predictor relationship according to rainfall amplitude, combined with the Bayesian model selection procedure, appear to be the best technique for forecasting seasonal rainfall in the Sahel.

## References


Andersen, I., Dione, O., Jarosewich-Holder, M., Olivry, J.C., 2005. The Niger River Basin: a vision for sustainable management. In: Golitzen, K.G. (Ed.), Directions in Development. The World Bank, Washington, DC, USA, p. 145.

Barry, D., Hartigan, J.A., 1993. A Bayesian analysis for change point problems. J. Am. Stat. Assoc. 88, 309–319.

Beaulieu, C., Ouarda, T.B.M.J., Seidou, O., 2005. Comparative study of homogenization techniques for precipitation data series. In: Progress Report No. 3 (Project on the Homogenization of Precipitation Data). Ouranos Consortium, Montreal (in French).

Beaulieu, C., Seidou, O., Ouarda, T.M.B.J., Zang, X., 2009. Intercomparison of homogenization techniques for precipitation data continued: comparison of two recent Bayesian change point models. Water Resour. Res. 45, http://dx.doi.org/10.1029/2008WR007501.

Begert, M., Thomas, S., Walter, K., 2005. Homogenous temperature and precipitation series of Switzerland from 1864 to 2000. Int. J. Climatol. 25 (1), 65–80.

Biasutti, M., Held, I.M., Sobel, A.H., Giannini, A., 2008. SST forcings and Sahel rainfall variability in simulations of the twentieth and twenty-first centuries. J. Clim. 21, 3471–3486.

Bouali, L., (Thèse de doctorat) 2009. Prévisibilité et prévision statistico-dynamique des saisons des pluies associées à la mousson ouest africaine à partir d'ensembles multi-modèles. Université de Bourgogne, France, 159 pp.

Brankovic, C., Palmer, T.N., 1997. Atmospheric seasonal predictability and estimates of ensemble size. Mon. Weather Rev. 125, 859–874.

Caminade, C., Terray, L., 2010. Twentieth century Sahel rainfall variability as simulated by the ARPEGE AGCM, and future changes. Clim. Dyn. 35, 75–94.

Christensen, J.H., et al., 2007. Regional climate projections in climate change 2007: the physical science basis. In: Solomon, S., et al. (Eds.), Contribution of Working Group I to the Fourth Assessment Report of the Intergovernmental Panel on Climate Change. Cambridge University Press, New York, pp. 847–940.

Descroix, L., Mahe, G., Lebel, T., Favreau, G., Galle, S., Gautier, E., Olivry, J.-C., Albergel, J., Amogu, O., Cappelaere, B., Dessouassi, R., Diedhiou, A., Breton, E.L., Mamadou, I., Sighomnou, D., 2009. Spatio-temporal variability of hydrological regimes around the boundaries between Sahelian and Sudanian areas of West Africa: a synthesis. J. Hydrol. 375, 90–102.

Ehsanzadeh, E., Adamowski, K., 2010. Trends in timing of low stream flows in Canada: impact of autocorrelation and long term persistence. Hydrol. Process. 24, 970–980.

Fearnhead, P., 2006. Exact and efficient Bayesian inference for multiple changepoint problems. Stat. Comput. 16, 203–213.

Gelfand, A.E., Hills, S.E., Racine-Poon, A., Smith, A.F.M., 1990. Illustration of Bayesian inference in normal data models using Gibbs sampling. J. Am. Stat. Assoc. 85, 972–985.

Giannini, A., Biasutti, M., Held, I.M., Sobel, A.H., 2008. A global perspective on African climate. Clim. Change 90, 359–383.

Hamatan, M., 2002. Synthèse et évaluation des prévisions saisonnières en Afrique de l'Ouest. DEA Sciences de l'Eau dans l'Environnement Continental. Université Montpellier 2, 115 pp.

Hansen, J.W., 2002. Realizing the potential benefits of climate prediction to agriculture: issues, approaches, challenges. Agric. Syst. 74 (3), 309–330.

Hansen, J.W., et al., 2011. Review of seasonal climate forecasting for agriculture in sub-Saharan Africa. Exp. Agric. 47 (2), 205–240.

Hastenrath, S., 1995. Recent advances in tropical climate prediction. J. Clim. 8, 1519–1532.

Hayes, M., Svoboda, M., LeComte, D., Redmond, K., Pasteris, P., 2005. Drought monitoring: new tools for the 21st century. In: Wihite, D.A. (Ed.), Drought and Water Crises: Science, Technology, and Management Issues. Taylor Francis, Boca Raton, LA, pp. 53–69.

Hunt, B.G., 2000. Natural climatic variability and Sahelian rainfall trends. Glob. Planet. Change 24, 107–131.

Ibrahim, B., Karambiri, H., Polcher, J., Yacouba, H., Ribsttein, P., 2014. Changes in rainfall regime over Burkina Faso under the climate change conditions simulated by 5 regional climate models. Clim. Dyn. 42, 1363–1381.

Janicot, S., Trzaska, S., Poccard, I., 2001. Summer Sahel-ENSO teleconnection and decadal time scale SST variations. Clim. Dyn. 18, 303–320.

Kumar, A., Hoerling, M., Ji, M., Leetmaa, A., Sardeshmukh, P., 1996. Assessing a GCM's suitability for making seasonal predictions. J. Clim. 9, 115–129.

Lopez-Bustins, J.A., Martin-Vide, J., Sanchez-Lorenzo, A., 2008. Iberia winter rainfall trends based upon changes in teleconnection and circulation patterns. Glob. Planet. Change 63, 171–176.

Lund, R., Reeves, J., 2002. Detection of undocumented changepoints: a revision of the two-phase regression model. J. Clim. 15, 2547–2554.

Mara, F., (Thèse de doctorat) 2010. Développement et analyse des critères de vulnérabilité des populations sahéliennes face à la variabilité du climat: le cas de la ressource en eau dans la vallée de la Sirba au Burkina Faso. Université du Québec à Montréal, 273 pp.
Min, S., Simonis, D., Hense, A., 2007. Probabilistic climate change predictions applying Bayesian model averaging. Philos. Trans. R. Soc. A 365, 2103–2116.
Mohino, E., Janicot, S., Bader, J., 2011. Sahel rainfall and decadal to multi-decadal sea surface temperature variability. Clim. Dyn. 37, 419–440.
Ogallo, L.A., Boulahya, M.S., Keane, T., 2000. Applications of seasonal to interannual climate prediction in agricultural planning and operations. Agric. For. Meteorol. 103, 159–166.
Palmer, T.N., 1986. Influence of the Atlantic, Pacific and Indian Oceans on Sahel rainfall. Nature 322, 251–253.
Palmer, T.N., Andersen, U., Cantelaube, P., Davey, M., Déqué, M., Diez, E., Doblas-Reyes, F.J., Feddersen, H., Graham, R., Gualdi, S., Guérémy, J.F., Hagedorn, R., Hoshen, M., Keenlyside, N., Latif, M., Lazar, A., Maisonnave, E., Marletto, V., Morse, A.P., Orfila, B., Rogel, P., Terres, J.M., Thomson, M.C., 2004. Development of a European multimodel ensemble system for seasonal-to-interannual prediction (DEMETER). Bull. Am. Meteorol. Soc. 85, 853–872.
Palmer, T.N., Brankovic, C., Richardson, D.S., 2000. A probability and decision-model analysis of PROVOST seasonal multi-model ensemble integrations. Q. J. R. Meteorol. Soc. 126, 2013–2034.
Perreault, L., Bernier, J., Bobee, B., Parent, E., 2000. Bayesian change-point analysis in hydrometeorological time series 2. Part 2. Comparison of change-point models and forecasting. J. Hydrol. 235, 242–263.
Philippon, N., Fontaine, B., 2002. The relationship between the Sahelian and previous 2nd Guinean rainy seasons: a monsoon regulation by soil wetness. Ann. Geophys. 20, 575–582.
Reeves, J., Chen, J., Wang, X.L., Lund, R., Lu, Q., 2006. A review and comparison of change point detection techniques for climate data. J. Appl. Meteorol. Climatol. 46, 900–914.
Rowell, D.P., 2001. Teleconnections between the tropical Pacific and the Sahel. Q. J. R. Meteorol. Soc. 127, 1683–1706.
Rowell, D.P., 2003. The impact of Mediterranean SSTs on the Sahelian rainfall season. J. Clim. 16, 849–862.
Samimi, C., Fink, A.H., Paeth, H., 2012. The 2007 flood in the Sahel: causes, characteristics and its presentation in the media and FEWS NET. Nat. Hazards Earth Syst. Sci. 12, 313–325.
Sarr, M.A., Zoromé, M., Seidou, O., Bryant, C.R., Gachon, P., 2013. Recent trends in selected extreme precipitation indices in Senegal-A changepoint approach. J. Hydrol., http://dx.doi.org/10.1016/j.jhydrol.2013.09.032.
Schepen, A., Wang, Q.J., Robertson, D.E., 2012. Combining the strengths of statistical and dynamical modeling approaches for forecasting Australian seasonal rainfall. J. Geophys. Res. 117, 148–227.
Seidou, O., Asselin, J.J., Ouarda, T.B.M.J., 2007. Bayesian multivariate linear regression with application to change-point models in hydrometeorological variables. Water Resour. Res., http://dx.doi.org/10.1029/2005WR004835.
Seidou, O., Ouarda, T.B.M.J., 2007. Recursion-based multiple changepoint detection in multiple linear regression and application to river streamflows. Water Resour. Res. 43, W07404, http://dx.doi.org/10.1029/2006WR005021.
Sittichok, K., Gado Djibo, A., Seidou, O., Saley, H.M., Karambiri, H., Paturel, J., 2014. Statistical seasonal rainfall and streamflow forecasting for the Sirba watershed, using sea surface temperature. Hydrol. Sci. J., http://dx.doi.org/10.1080/02626667.2014.944526.
Tarhule, A., 2005. Damaging rainfall and flooding: the other Sahel Hazards. Clim. Change 72 (3), 355–377.
Taweye, A., (Dissertation) 1995. Contribution à l'étude hydrologique du bassin versant de la Sirba à Garbé-Kourou. Centre Régional AGRHYMET, 96 pp.
Thiaw, W., Barnston, A.G., Kumar, V., 1999. Predictions of African rainfall on the seasonal time scale. J. Geophys. Res. 104, 31589–31597.
Villarini, G., Smith, J.A., Serinaldi, F., Ntelekos, A.A., 2011. Analyses of seasonal annual and maximum daily discharge records for central Europe. J. Hydrol. 399, 299–312.
Vincent, L.A., 1998. A technique for the identification of inhomogeneities in Canadian temperature series. J. Clim. 11, 1094–1105.
Xiong, L., Guo, S., 2004. Trend test and change-point detection for the annual discharge series of the Yangtze River at the Yichang hydrological station. Hydrol. Sci. J. 49 (1), 99–112.